Nanostructural and biochemical property changes in activation-induced CD8+ T cell apoptosis utilizing AFM and Raman spectroscopy

Y.J. Lee[1], G.J. Lee[1,2] and H.K. Park[1,2,*]

[1]Dept. of Biomedical Engineering & Healthcare Industry Research Institute, College of Medicine, Kyung Hee University, Seoul, Korea, jaya21@hanmail.net
[2]Dept. of Medical Engineering, Graduate School, Kyung Hee University, Seoul, Korea, gjlee@khu.ac.kr, sigmoidus@khu.ac.kr

ABSTRACT

This study was to investigate the the morphological and biochemical property changes at a molecular level in resting and activated T cell using atomic force microscopy (AFM) and Raman spectroscopy. We investigated the nanostructural alterations in T cell activation isolated from the spleens of C57BL/6 mice by positive selection using CD8a MicroBeads using AFM & Raman spectroscopy. All peaks were significantly decreased when the CD8+ T cells were stimulated with CD3/CD28 as compared to resting cells by Raman spectroscopy. The cell volume and perimeter of activated CD8+ T cells significantly increased over those in the resting state. The surface roughness parameters of activated CD8+ T cells significantly increased over those of resting CD8+ T cells. Our findings regarding the nanostructural and biochemical changes observed in activated CD8+ T cells by AFM and Raman spectroscopy will provide new informations in the area of nanomedicine for the treatment of T cell related immunity.

Keywords: Atomic force microscopy, Raman spectroscopy, CD8+ T cell, Activation

1 INTRODUCTION

T-cell activation is one of the important affairs in immune response and an area of extensive research. Activated T cell show morphological and biochemical change both inside the cell and on the cell surface. However, to date, there have been few studies of the biophysical and nanostructural alteration of T cell activation. Currently, the most commonly used technique to identify these changes is fluorescence-activated cell sorting (FACS) analysis. It is depend on labeling cells with fluorochrome conjugated antibodies specific for molecules of interest to assess their activation status. For fluorescence-based methods, broad emission spectra from molecular fluorochrome make multiplexing impossible, and the disadvantage of their susceptibility to photobleaching may greatly weaken their detection limits.

In contrast, Raman spectroscopy for biomolecules can overcome some of the limitations of fluorescence spectroscopy in terms of photostability and spectral multiplexing. This technique has attracted great interest as a powerful analytical tool that can be used to detect changes in the structure and composition of analytes at the molecular level [1-3]. Atomic force microscopy (AFM)-based techniques offer advanced and elegant methods for characterizing surface properties as well as changes to the mechanical properties of the cell membrane [4-6]. AFM, which is a type of high-resolution scanning probe microscopy, is a powerful tool for imaging at the nanometer level and for observing cellular ultrastructures [7, 8].

The aim of this study is to investigate the morphological and biochemical property changes at a molecular level in resting and activated T cell using AFM and Raman spectroscopy.

2 MATERIALS AND METHODS

2.1 Animals

C57BL/6 mice (6–8 wk, 20–25 g) were purchased from Orient Bio Korea (Seoul, South Korea). All animal use procedures were approved by the Ethical Committee of the Kyung Hee University School of Medicine, and were in strict accordance with the National Institutes of Health Guide for the Care and Use of Laboratory Animals..

2.2 Chemicals and Antibodies

CD8a MicroBeads were purchased from Miltenyi Biotec (Bergisch-Gladbach, Germany). Anti-mouse CD3 and anti-mouse CD28 antibodies were purchased from BD Biosciences (San Jose, CA). Anti-mouse CD8a-PE and anti-mouse CD137 (4-1BB)-PE antibodies were purchased from eBioscience (San Diego, CA). Cell-Tak cell and tissue adhesives were purchased from BD Biosciences (San Jose, CA)..

2.3 CD8+ T cell Isolation and Activation

CD8+ T cells were isolated from the spleens of C57BL/6 mice by positive selection using CD8a MicroBeads. The purity of the populations were determined by flow cytometry, and routinely reached ≥ 93%. For cell activation, cells ($1\text{-}2\times10^5$) were seeded on a 60 mm dish coated with anti-mouse CD3 antibody and then treated with anti-mouse CD28 antibody.

2.4 Flow cytometry Analysis

Isolated CD8+ T cells were incubated with an optimal concentration of anti-mouse CD8a-PE for 30 min at 4˚C in the dark. Cells were washed three times and resuspended in flow cytometry staining buffer (eBioscience, San Diego, CA), and the percentage of cells stained with a particular set of reagents was analyzed using a FACS Calibur with CellQuest software (BD Biosciences, San Jose, CA). For the confirmation of CD8+ T cell activation, cells were treated with anti-mouse CD137 (4-1BB)-PE and then resuspended in flow cytometry staining buffer. Flow cytometric analysis was immediately performed.

2.5 Raman Spectroscopic Measurements

For Raman analysis of CD8+ T cells, CD8+ T cells were seeded in gold-coated substrates and incubated for 24 hr. The CD8+ T cells were washed twice with filtered PBS and fixed for 20 min in 4% paraformaldehyde in PBS at 4 °C, followed by a final wash with 5 ml PBS. In order to minimize spectral contributions from the sample substrate, we used gold-coated substrate. Pure metals are known to have no Raman spectral features and very low background signal. Raman spectra were acquired using the SENTERRA confocal Raman system (Bruker Optics Inc., Billerica, MA, USA) equipped with a 785 nm diode laser source (100 mW before objective) and a resolution of 3 cm^{-1}. A 100× air objective (MPLN N. A. 0.9, Olympus), which produced a laser spot size of ~ 1μm was used to collect Raman signals and focus the laser on a single cell. The Raman spectra of cells and DNA were calculated as the average of fifteen measured samples. All Raman measurements are recorded with an accumulation time of 60s in the 600-1750 cm^{-1} range, and spectral acquisitions were carried out using the OPUS software.

2.6 AFM Measurements

Nanoscale morphological changes in CD8+ T cells were investigated using an AFM system (Surface Imaging Systems, Herzogenrath, Germany). Non-contact mode AFM images were obtained using a NANOS N8 NEOS (Bruker, Herzogenrath, Germany) equipped with a 42.5 × 42.5 × 4 μm^3 XYZ scanner and two Zeiss optical microscopes (Epiplan 200× and 500×). External noise was eliminated by placing the AFM on an active vibration isolation table (Table Stable Ltd., Surface Imaging Systems, Herzogenrath, Germany) inside a passive vibration isolation table (Pucotech, Seoul, Republic of Korea). The CD8+ T cells were scanned at a resolution of 512 × 512 pixels, with a scan rate of 0.6 lines/sec. The shape parameters, including perimeter and volume, and roughness parameters of the cells were measured from the topographic images using the Scanning Probe Imaging Processor (SPIP™, Image Metrology, Hørsholm, Denmark). The average surface roughness (Sa) is defined as the arithmetic mean of the deviations in height from the mean value, and Sq is the root mean square. Fifty different areas randomly selected 1 × 1 μm^2 sections of the cell membrane.

3 RESULTS

Figure 1A showed that CD8+ T cells were isolated from splenocytes with more than 93% purity by flow cytometric analysis. The activated CD8+ T cells became larger and more spherical than resting CD8+ T cells (Figure 1B). The expression of CD137 on activated CD8+ T cells also increased in comparison with resting CD8+ T cells (Figure 1C). Therefore, we confirmed that isolated CD8+ T cells were effectively activated with anti-mouse CD3 antibody and anti-mouse CD28 antibody.

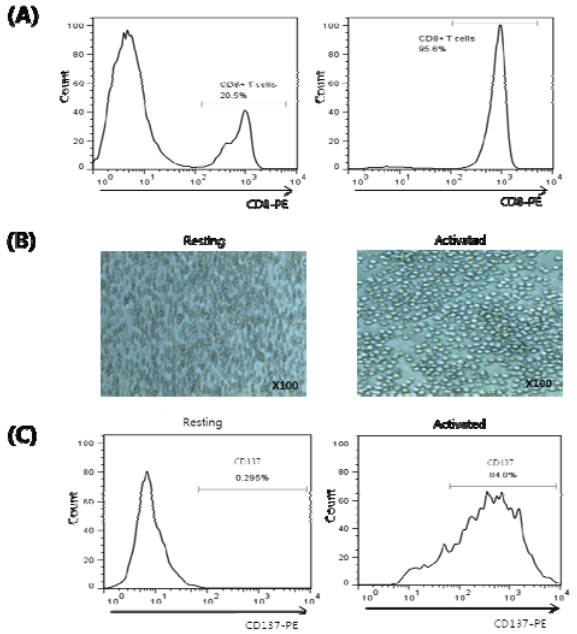

Figure 1. (A) CD8+ T cells were isolated from mouse splenocytes using PE-labeled anti-CD8a mAb and anti-PE microbeads. (B) CD8+ T cells were stimulated with anti-CD3 mAb plus anti-CD28 mAb for three days. Morphological images were collected using an optical microscopy system (100×). (C) The surface marker CD137 was analyzed in activated CD8+ T cells by flow cytometry analysis.

The averaged Raman spectra of resting and activated CD8+ T cells are presented in Figure 2 (curve a: resting, curve b: activated). It is evident that both the resting and the activated CD8+ T cells exhibit spectra corresponding to molecular vibrations of all cellular components, including nucleic acids, proteins, lipids and carbohydrates [9-11]. In order to quantitatively identify the effect of activation maturation on the CD8+ T cells, we selected some specific Raman spectra and compared the changes in their spectral

intensities. The main changes related to the protein vibration can be observed at 1002 cm^{-1} (symmetric ring stretching phenylalanine), and 1234 cm^{-1} (amide III β–sheet of protein). The changes of Raman spectra intensity corresponded to DNA vibration at 725 cm^{-1} (adenine), 778 cm^{-1} (cytosine/thymine ring breathing of the DNA/RNA), and 1096 cm^{-1} (phosphodioxy groups, PO_2^- , of the DNA backbone).

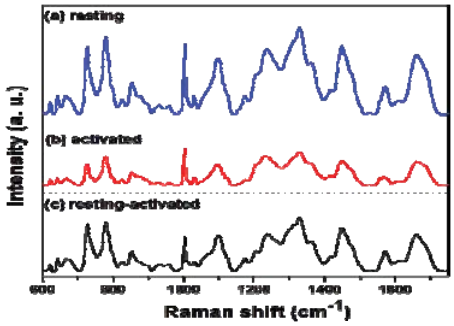

Figure 2. Averaged Raman spectra of CD8+ T cells: (a) resting and (b) activated. (c) The spectrum shows the spectral differences of resting and activated CD8+ T cells.

Figure 3 shows representative 3-dimensional AFM topographic images and line profiles of resting and activated CD8+ T cells. As shown in Figure 3, there were significant structural changes in CD8+ T cells after activation. In comparison with resting CD8+ T cells (Figure 3A), there were increases in cell size, surface roughness, and irregularity of the cellular rim in activated CD8+ T cells (Figure 3B). Cell height, which was defined as the difference between the top and bottom of the cell, was determined from the AFM topographic images. The height of the CD8+ T cells was not statistically different between resting and activated CD8+ T cells.

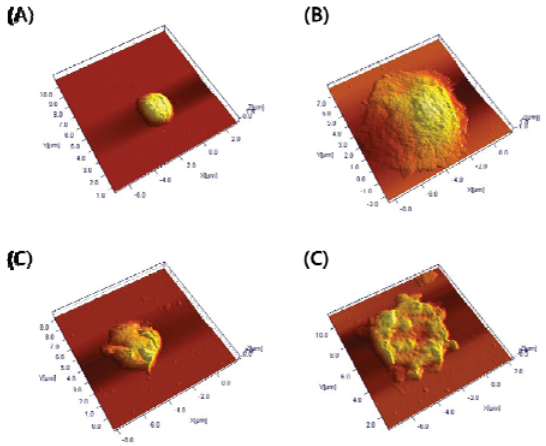

Figure 3. Figure 4. Representative 3D-modified AFM topographic images (10 μm × 10 μm) of the (A) resting and (B) activated T cells, as well as Zap70 siRNA treated (C) resting and (D) activated T cells.

To identify the morphological changes between resting and activated CD8+ T cells, surface roughness were evaluated. The cell volume of activated CD8+ T cells significantly increased from 12.40 ± 1.95 μm^3 (resting CD8+ T cells) to 31.20 ± 8023 μm3 (activated CD8+ T cells) ($p<0.0001$, n=5). The cell perimeter of activated CD8+ T cells was increased over those in the resting state (19.87 ± 1.81 μm vs. 34.93 ± 2.23 μm, $p<0.0001$, n=5). Therefore, there was a significant change in cell perimeter between resting and activated CD8+ T cells. Additionally, the surface roughness parameters of activated CD8+ T cells significantly increased to 28.48 ± 14.99 nm for Sa ($p<0.001$, n=30), comparing with those of resting CD8+ T cells (21.38 ± 7.74 nm for Sa).

4 DISCUSSION

In this study, we investigated morphological and biochemical property changes at a molecular level in resting and activated CD8+ T cell using AFM and Raman spectroscopy. The band at 778 cm^{-1} is assigned to the ring breating mode of the DNA bases cytosine and thymine and the RNA base uracil. The main changes related to the proteins can be observed at 1002, and 1659 cm^{-1}. The sharp band at 1002 cm^{-1} corresponds to the ring stretching of phenylalanine, which is very important component of proteins. It has been shown that this peak is very sensitive to the death of cells [9, 12, 13]. The peak at 1656 cm^{-1} represents amid I (α-helix), which is basic component of protein structure and is also extremely sensitive to changes in the structure of the protein. The 1097 cm^{-1} peak represents the vibrations of the phosphodioxy groups PO_2^- in the DNA/RNA backbone. The peak at 1449 cm^{-1} can be attributed to DNA, proteins and lipids. For activated CD8+ T cell, the reduction in Raman intensities corresponding to DNA, such as 778 (62 %) and 1097 cm^{-1} (63 %), arose from the destruction of the ring structures, indicating degradation of the DNA. Furthermore, the decrease in the magnitude of Raman intensities corresponding to proteins, such as 1002 (48 %) and 1659 cm^{-1} (60 %), suggests denaturation and conformational changes of proteins. These findings indicate that Raman spectroscopy can be used as label-free and noninvasive optical technique to reveal the activation status of CD8+ T cells.

AFM is a powerful nanotechnology tool which can identify the surface properties, as well as changes to the mechanical properties, of cell membranes [14-16]. However, there have only been a few studies of T cells to have utilized AFM technology. This technique also allows for the quantitative analysis of the biophysical properties of T cell activation. It was confirmed that the activation of CD8+ T cells results in an increased cell volume and cell perimeter (that is, a more irregular rim shape) over that observed in resting CD8+ T cells.

It is hypothesized that this change in AFM and Raman spectroscopy during the activation of CD8+ T cells might

be a result of rearrangement of the structure of the cell, as well as the activated cell metabolism [17]. However, more research is needed to determine the exact mechanism of the findings of this study.

5 CONCLUSION

In conclusion, our findings regarding the nanostructural and biochemical changes observed in activated CD8+ T cells by AFM and Raman spectroscopy will provide new informations in the area of nanomedicine for the treatment of T cell related immunity. As far as we know, this is the first study to identify nanostructural changes to CD8+ T cells in activated state using by AFM and Raman spectroscopy.

ACKNOWLEDGEMENTS

This work was supported by the Technology Innovation Program (Grant No. 10054687) funded by the Ministry of Trade, Industry & Energy.

REFERENCES

[1] S. Dochow, C. Krafft, U. Neugebauer, T. Bocklitz, T. Henkel, G. Mayer, J. Albert and J. Popp, "Tumour cell identification by means of Raman spectroscopy in combination with optical traps and microfluidic environments", Lab on a chip, 11, 1484-1490, 2011.

[2] W.A. El-Said, T.H. Kim, H. Kim and J.W. Choi, "Analysis of intracellular state based on controlled 3D nanostructures mediated surface enhanced Raman scattering", PloS one, 6, e15836, 2011.

[3] M.M. Mariani, P.J. Day and V. Deckert, "Applications of modern micro-Raman spectroscopy for cell analyses", Integrative biology : quantitative biosciences from nano to macro, 2, 94-101, 2010.

[4] M. Xu, D. Fujita, K. Onishi and K. Miyazawa, "Improving accuracy of sample surface topography by atomic force microscopy" Journal of nanoscience and nanotechnology, 9, 6003-6007, 2009.

[5] G.J. Lee, S. Choi, J. Chon, S. Yoo, I. Cho and H.K. Park, "Changes in collagen fibril pattern and adhesion force with collagenase-induced injury in rat Achilles tendon observed via AFM", Journal of nanoscience and nanotechnology, 11, 773-777, 2011.

[6] W.A. Lam, M.J. Rosenbluth and D.A. Fletcher, "Chemotherapy exposure increases leukemia cell stiffness", Blood, 109, 3505-3508, 2007.

[7] G. Binnig, C.F. Quate and C. Gerber, "Atomic force microscope", Physical review letters, 56, 930-933, 1986.

[8] S.S. Schaus and E.R. Henderson, "Cell viability and probe-cell membrane interactions of XR1 glial cells imaged by atomic force microscopy", Biophysical journal, 73, 1205-1214, 1997.

[9] I. Notingher, J. Selvakumaran and L.L. Hench, "New detection system for toxic agents based on continuous spectroscopic monitoring of living cells", Biosensors & bioelectronics, 20, 780-789, 2004.

[10] Q. Matthews, A. Jirasek, J. Lum, X. Duan and A.G. Brolo, "Variability in Raman spectra of single human tumor cells cultured in vitro: correlation with cell cycle and culture confluency", Applied spectroscopy, 64, 871-887, 2010.

[11] J.W. Chan, D.S. Taylor, T. Zwerdling, S.M. Lane, K. Ihara and T. Huser, "Micro-Raman spectroscopy detects individual neoplastic and normal hematopoietic cells", Biophysical journal, 90, 648-656, 2006.

[12] C.A. Owen, J. Selvakumaran, I. Notingher, G. Jell, L.L. Hench and M.M. Stevens, "In vitro toxicology evaluation of pharmaceuticals using Raman micro-spectroscopy", Journal of cellular biochemistry, 99, 178-186, 2006.

[13] I. Notingher, C. Green, C. Dyer, E. Perkins, N. Hopkins, C. Lindsay and L.L. Hench, "Discrimination between ricin and sulphur mustard toxicity in vitro using Raman spectroscopy", Journal of the Royal Society, Interface / the Royal Society, 1, 79-90, 2004.

[14] M. Xu, D. Fujita, K. Onishi and K. Miyazawa, "Improving accuracy of sample surface topography by atomic force microscopy", Journal of nanoscience and nanotechnology, 9, 6003-6007, 2009.

[15] G.J. Lee, S. Choi, J. Chon, S. Yoo, I. Cho and H.K. Park, "Changes in collagen fibril pattern and adhesion force with collagenase-induced injury in rat Achilles tendon observed via AFM", Journal of nanoscience and nanotechnology, 11, 773-777, 2011.

[16] W.A. Lam, M.J. Rosenbluth and D.A. Fletcher, "Chemotherapy exposure increases leukemia cell stiffness", Blood, 109, 3505-3508, 2007.

[17] Y. Wu, H. Lu, J. Cai, X. He, Y. Hu, H. Zhao and X. Wang, "Membrane Surface Nanostructures and Adhesion Property of T Lymphocytes Exploited by AFM", Nanoscale research letters, 4, 942-947, 2009.